Synthesis, characterization, and solution structure of all-conjugated polyelectrolyte diblock copoly(3-hexylthiophene)s

Hao Xia,[a] Zhi Ye,[a] Xiaofeng Liu,[b] Juan Peng*[a] and Feng Qiu*[a]

We report on a new class of all-conjugated polyelectrolyte diblock copoly(3-hexylthiophene)s, poly(3-hexylthiophene)-*b*-poly[3-[6-(*N*-methylimidazolium)hexyl]thiophene] (P3HT-*b*-P3MHT). The polyelectrolyte diblock copolymers were prepared by a catalyst-transfer Kumada polycondensation followed by quaternization of the bromohexyl side groups of the poly[3-(6-bromohexyl)thiophene] block with *N*-methylimidazole. The obtained diblock copolymers have well-defined block ratios, narrow polydispersity indices, and high regioregularity. Their characterization as well as the thermal, crystalline, and optical properties, and self-assembly behavior have been investigated in detail. Transmission electron microscopy (TEM) provided evidence for solvent-induced self-assembly. A series of morphologies including short or long nanowires and nanorings could be obtained depending on the selectivity of solvents toward different blocks and the block ratios.

Introduction

Conjugated polymers have gained immense interest over the past few years due to their promising applications in organic electronics such as in photovoltaic cells,[1–3] organic field-effect transistors,[4] and light emitting diodes.[5] Among various conjugated polymers, regioregular poly(3-alkylthiophene)s (P3ATs) are one of the most widely studied semiconducting polymers because of their excellent charge carrier mobility, and chemical stability, as well as their facile preparation.[6] Since the optoelectronic properties of P3ATs are closely related to their molecular packing and morphology on the nanometer scale, controlling their structures by various methods is important for further improvements in device performance. One of the fascinating routes to control the nanostructure is to design block copolymers with P3ATs, which can self-organize into well-defined microphase-separated structures on the nanometer scale. A variety of P3AT-based rod-coil block copolymers have been designed and synthesized using a grafting-from approach or a grafting-to approach, such as poly(3-hexylthiophene)-*b*-poly(vinylpyridine) (P3HT-*b*-PVP),[7] poly(3-hexylthiophene)-*b*-poly(methyl methacrylate) (P3HT-*b*-PMMA),[8,9] and poly(3-alkylthiophene)-*b*-poly(ethylene oxide) (P3AT-*b*-PEO).[10–12] However, those coil blocks are usually insulating which only support the self-assembly but would lead to the decline in total electronic properties. As such, the research on all-conjugated

rod–rod block copolymers has become a focus of interest because they combine the optoelectronic properties of conjugated polymers with the fascinating self-assembly properties of block copolymers.[13–29] For example, Tu *et al.* reported the first amphiphilic all-conjugated diblock copolymer poly[9,9-bis(2-ethylhexyl)fluorene]-*b*-poly[3-(6-diethylphosphonatohexyl)thiophene] (PF2/6-*b*-P3PHT), which showed vesicle formation in mixtures of non-selective and selective solvents.[14] Wu *et al.* reported the first example of a polythiophene-*b*-polypeptide diblock copolymer, poly(3-hexylthiophene)-*b*-poly(γ-benzyl-L-glutamate) (P3HT-*b*-PBLG), which can self-assemble into hierarchal structures in solution and in the solid state.[15] Hollinger *et al.* reported a new class of copolymer poly(3-hexylselenophene)-*b*-poly(3-hexylthiophene) (P3HS-*b*-P3HT) and discovered that phase separation as well as the optical properties could be controlled by the heterocycle in the polymer chain.[16] Iovu *et al.*, Wu *et al.*, and our group reported a series of poly(3-alkylthiophene)-*b*-poly(3-alkylthiophene) (P3AT-*b*-P3AT) diblock copolymers in which the side alkyl groups were different.[17–22] These different alkyl groups endowed P3ATs with different physical properties such as solubility, melting point, and crystallinity and the interplay between the crystallization and microphase separation of these diblock copoly(3-alkylthiophene)s were investigated.

Conjugated polyelectrolytes (CPEs), which contain π-conjugated backbone and pendant ionic groups, show unique optical and electrical properties together with good solubility in polar solvents. They can be used as charge (electron) injection layers in various optoelectronic applications.[30] As these CPEs may also be water soluble, they are advantageous because they do not damage the underlying organic soluble polymer film. Another

[a]*State Key Laboratory of Molecular Engineering of Polymers, Department of Macromolecular Science, Fudan University, Shanghai 200433, China. E-mail: juanpeng@fudan.edu.cn; fengqiu@fudan.edu.cn*

[b]*Department of Chemistry, Fudan University, Shanghai 200433, China*

possible application of CPEs is chemical and biological sensing based on the conformational changes of CPEs when complexed with other charged species.[31,32]

All-conjugated polyelectrolyte block copolymers are the combination of CPEs and all-conjugated block copolymers. With the advantage of both, several all-conjugated polyelectrolyte block copolymers have been introduced by Scherf *et al.*, including poly[9,9-bis(2-ethylhexyl)fluorene]-*b*-poly[3-(6-trimethyl-ammoniumhexyl)thiophene] (PF2/6-*b*-P3TMAHT),[33] poly[9,9-bis(2-ethylhexyl)fluorene]-*b*-poly [3-(6-pyridylhexyl)-thiophene] (PF2/6-*b*-P3PyHT), and poly[9,9-bis(6-trimethyl-ammoniumhexyl)-2,7-fluorene]-*b*-poly(9,9-bisoctyl-2,7-fluorene) (PF6NBr-*b*-PF8),[34] *etc.* These polyelectrolyte block copolymers were generated in a grafting from approach starting from an end-functionalized polythiophene as a macroinitiator or Suzuki-Miyaura type polycondensation method. Up to now, all-conjugated polyelectrolyte block copolymers reported until today are very limited. Although a series of all-conjugated P3AT-*b*-P3AT diblock copolymers have been synthesized and investigated, their polyelectrolyte type is still lacking.

Herein, we report a new class of all-conjugated polyelectrolyte diblock copoly(3-hexylthiophene)s, poly(3-hexylthiophene)-*b*-poly[3-[6-(*N*-methylimidazolium)hexyl]thiophene] (P3HT-*b*-P3MHT), which contains only poly(3-hexylthiophene) as the copolymer backbone. Poly(3-hexylthiophene) is one block and its derivative with pendant ionic *N*-methylimidazole is the other block. To the best of our knowledge, this represents the first example of an all-conjugated polyelectrolyte diblock copoly(3-alkylthiophene)s. Of particular interest to us is that only the difference in their side chains of two blocks is expected to lead to some intriguing physical properties. We also demonstrate whether such all-conjugated polyelectrolyte diblock copoly(3-hexylthiophene)s of distinct block ratios crystallize in a distinct matter, and how the solvent influences the copolymer structure.

Experimental

Materials

The monomers 2-bromo-5-iodo-3-hexylthiophene (M_1) and 2-bromo-5-iodo-3-bromohexylthiophene (M_2) were synthesized according to the literature.[35] Isopropylmagnesium chloride (i-PrMgCl, 2.0 M in tetrahydrofuran) and (1,3-bis(diphenylphosphino)-propane)-dichloronickel(II) (Ni(dppp)Cl$_2$) were purchased from Aldrich and used as received. *N*-methylimidazole (99%) was purchased from J&K Scientific Ltd. and used as received. The other reagents and solvents were purchased from Sinopharm Chemical Reagent Co., Ltd. (SRC). Tetrahydrofuran (THF) was freshly dried over sodium benzophenone ketyl, and all other solvents were used as received.

Synthesis of poly(3-hexylthiophene)-*b*-poly[3-(6-bromohexyl)-thiophene], (P3HT-*b*-P3BrHT)

P3HT-*b*-P3BrHT was synthesized by a catalyst-transfer Kumada polycondensation. The molar feed ratios of M_1 to M_2 in the polymerization of P3HT-*b*-P3BrHT were 3 : 1, 1 : 1, and 1 : 3.

The typical synthesis procedure of the P3HT-*b*-P3BrHT with the feed molar ratio of 1 : 1 was as follows: M_1 (0.8952 g, 2.4 mmol) was dissolved in THF (50 mL) in a three-neck flask and stirred under N_2. After cooling the solution to 0 °C, *i*-PrMgCl in THF (1.2 mL, 2.4 mmol) was added *via* a syringe and the mixture was stirred for 30 min. Then the solution was heated to 35 °C and followed by the addition of Ni(dppp)Cl$_2$ catalyst (54.2 mg, 0.1 mmol). The resulting mixture was stirred at 35 °C for 30 min. Meanwhile, M_2 (1.0848 g, 2.4 mmol) in another flask was reacted with *i*-PrMgCl (1.2 mL, 2.4 mmol) at 0 °C for 30 min. After 30 min reaction, the second solution was added to the first one and the resulting mixture was reacted at 35 °C for 4 h. The reaction was quenched by adding HCl (aq.) (50 wt%), and the product was precipitated into methanol and hexane and dried under vacuum to give a purple solid (0.77 g, 79%). P3HT-*b*-P3BrHT with the molar ratios of 3 : 1 and 1 : 3 were synthesized in the same way. Based on the ratio of the integration areas of the two peaks at 0.94 and 3.43 ppm assigned to the resonances of terminal methyl group in hexyl side chain and bromomethyl group in 6-bromohexyl side chain derived from ^{1}H NMR spectra, the actual molar ratios of the P3HT and P3BrHT blocks were calculated to be 3 : 1.29, 1 : 1.12, and 1 : 3.19, respectively. ^{1}H NMR (500 MHz, CDCl$_3$, δ(ppm)): 7.01 (1H), 3.43 (1.10H), 2.82 (1.95H), 1.91 (1.15H), 1.72 (1.15H), 1.55–1.37 (4.96H), 0.94 (1.48H).

Synthesis of poly(3-hexylthiophene)-*b*-poly[3-[6-(*N*-methylimidazolium)hexyl]thiophene] (P3HT-*b*-P3MHT)

P3HT-*b*-P3MHT was synthesized by quaternization of the bromohexyl side groups of P3HT-*b*-P3BrHT with *N*-methylimidazole. The obtained P3HT-*b*-P3BrHT (0.10 g) was dissolved in chloroform (10 mL) and *N*-methylimidazole (0.38 mL, 4.86 mmol) was added to the solution. The mixture was stirred at 90 °C for 48 h. The mixture was poured into ether to obtain the crude product. After filtration, the crude product was washed with excess ether and dried under vacuum to give the P3HT-*b*-P3MHT product of 0.081 g (68% yield). ^{1}H NMR (400 MHz, CDCl$_3$, δ(ppm)): 10.02, 7.73, 6.97, 4.34, 4.06, 2.79, 1.91–1.25, 0.86.

Synthesis of homopolymer poly[3-[6-(*N*-methylimidazolium)-hexyl]thiophene] (P3MHT)

P3MHT was also synthesized in a similar two stages: synthesis of poly[3-(6-bromohexyl)thiophene] (P3BrHT) followed by quaternization of the bromohexyl side groups of P3BrHT with *N*-methylimidazole. M_2 (2.26 g, 5.0 mmol) was dissolved in THF (50 mL) in a three-neck flask and stirred under N_2. After cooling the solution to 0 °C, *i*-PrMgCl in THF (2.5 mL, 5 mmol) was added and the mixture was stirred for 30 min. Then the solution was heated to 35 °C and followed by the addition of Ni(dppp)Cl$_2$ catalyst (0.1356 g, 0.25 mmol). The resulting mixture was stirred at 35 °C for 4 h. The reaction was quenched by adding HCl (aq.) (50 wt%), and the product was precipitated into methanol and hexane and dried under vacuum to give a red solid (M_n = 4700 g mol^{-1}, PDI = 1.26). The obtained P3BrHT (0.10 g) was dissolved in chloroform (10 mL) and *N*-methylimidazole (0.65 mL, 8.16

mmol) was added to the solution. The mixture was stirred at 90 °C for 48 h. The mixture was poured into ether to obtain the crude product. After filtration, the crude product was washed with excess ether and dried under vacuum to give the P3MHT product. ^{1}H NMR (500 MHz, CD$_3$OD, δ(ppm)): 7.66 (m, 1H), 7.58 (m, 1H), 7.10 (bs, 1H), 4.25 (bs, 2H), 3.93 (s, 3H), 2.87 (bs, 2H), 1.94 (m, 2H) 1.74 (m, 2H), 1.50–1.43 (m, 4H).

Characterization

Gel permeation chromatography (GPC) was operated using an Agilent 1100 system equipped with both G1362A refractive-index and G1314A UV detectors (eluent: THF; calibration: polystyrene standards). ^{1}H NMR spectra were recorded on a DMX500 MHz spectrometer in CDCl$_3$ or CD$_3$OD with tetramethylsilane (TMS) as the internal standard. Differential scanning calorimetry (DSC) thermograms and thermogravimetric (TGA) analysis were measured using TA DSC Q2000 at a heating rate of 10 °C min^{-1} under N$_2$ flow and TE Pyris 1 TGA, respectively. UV-vis absorption spectra were recorded on Perkin Elmer Lambda 35 UV-vis spectrophotometers. X-ray diffraction (XRD) was performed on a PANalytical X'Pert PRO X-ray diffractometer using Cu Kα radiation (λ = 1.541 Å) operating at 40 kV and 40 mA. The samples for XRD measurements were prepared by drop-casting 10 mg mL^{-1} polymer solutions onto silicon wafers. Transmission electron microscope (TEM) imaging was performed on a Tecnai G^2 20-Twin transmission electron microscope operated at 200 kV. As for TEM analysis, the samples were prepared by drop-casting 1 mg mL^{-1} copolymer solutions on copper grids, followed by evaporation of the solvent at ambient.

Results and discussion

Synthesis and characterization of P3HT-b-P3MHT diblock copolymer

The synthetic route to P3HT-b-P3MHT diblock copolymer is depicted in Scheme 1. The P3HT-b-P3BrHT was synthesized by catalyst-transfer Kumada polycondensation with two steps. In the first step, the P3HT block was polymerized from activated monomer 2-bromo-5-iodo-3-hexylthiophene to obtain the end living P3HT polymers. In the second step, the other activated monomer 2-bromo-5-iodo-3-bromohexylthiophene was added to the reacting solution to obtain the diblock copolymer P3HT-b-P3BrHT. The target polyelectrolyte diblock copolymer P3HT-b-P3MHT was finally achieved in high yields via quaternization of copolymer P3HT-b-P3BrHT with N-methylimidazole in chloroform.
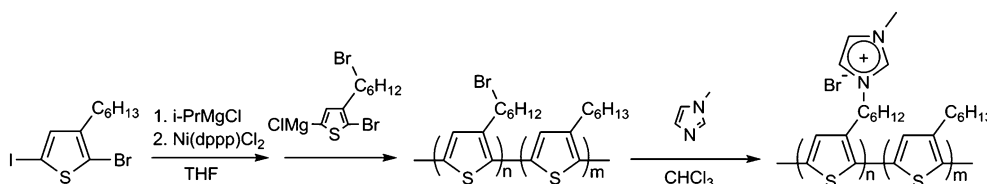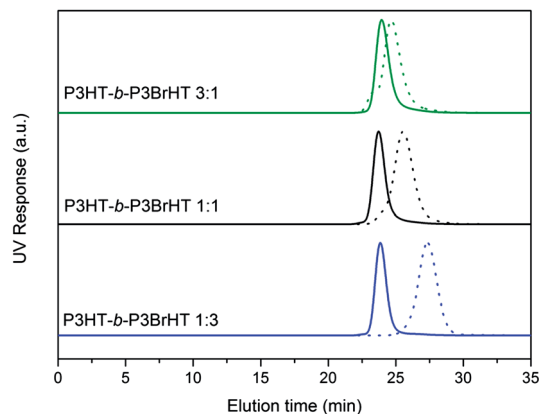

Fig. 1 GPC profiles of P3HT-b-P3BrHT diblock copolymers. Dashed lines represent the GPC profiles of P3HT synthesized in the first step and solid lines show the GPC profiles of the P3HT-b-P3BrHT diblock copolymers after the second-stage polymerization without quaternization.

Fig. 1 displays the GPC profiles of P3HT synthesized in the first step and the diblock copolymer P3HT-b-P3BrHT after the second-step polymerization without quaternization. Compared to the peaks of the P3HT obtained in the first step, the peaks of the P3HT-b-P3BrHT all shift to a higher molecular weight with the maintenance of the single peak. The molar feed ratios of monomers M1 to M2 and the resulting P3HT-b-P3BrHT block copolymers with different ratios of two blocks are summarized in Table 1. The molecular weight of P3HT block is varied from 2000 g/mol to 8000 g mol^{-1}. The block copolymers P3HT-b-P3BrHT all show relatively high molecular weight from 11 600 g mol^{-1} to 13 600 g mol^{-1} and narrow PDI of 1.04–1.12, as shown in Table 1.

In comparison to the ^{1}H-NMR spectrum of P3HT-b-P3BrHT (Fig. 2), new signals at δ = 10.02 and 7.73 ppm appeared in final product P3HT-b-P3MHT, which are attributed to the protons at 2- and 4-/5- positions of the imidazole ring, while the other new peaks at δ = 4.34 and 4.06 ppm correspond to the α-protons of hexyl group close to the imidazole ring and the methyl group on the imidazole ring. Moreover, the signal at δ = 3.43 in P3HT-b-P3BrHT disappeared, indicating the removal of bromide and the accomplished reaction between P3HT-b-P3BrHT and N-methylimidazole.

Thermal analysis

To investigate the thermal properties of the polyelectrolyte diblock copolymer P3HT-b-P3MHT, all the polymers including

Scheme 1 Synthesis route of P3HT-b-P3MHT polyelectrolyte diblock copoly(3-hexylthiophene)s.

Table 1 Summary of compositions, molecular weights and PDI of P3HT-*b*-P3BrHT diblock copolymers

Polymer	Feed molar ratio (M1 : M2)	m/n^a (%)	$M_{n,P3HT}$ (g mol^{-1})	$M_{n,total}$ (g mol^{-1})	PDI
P3HT-*b*-P3BrHT	3 : 1	70 : 30	8000	11 600	1.12
	1 : 1	47 : 53	5300	13 400	1.11
	1 : 3	24 : 76	2000	13 600	1.04

[a] Determined by ^{1}H NMR. *m,n*: the molar amount of the P3HT and the P3BrHT block in the synthesized P3HT-*b*-P3BrHT, respectively.
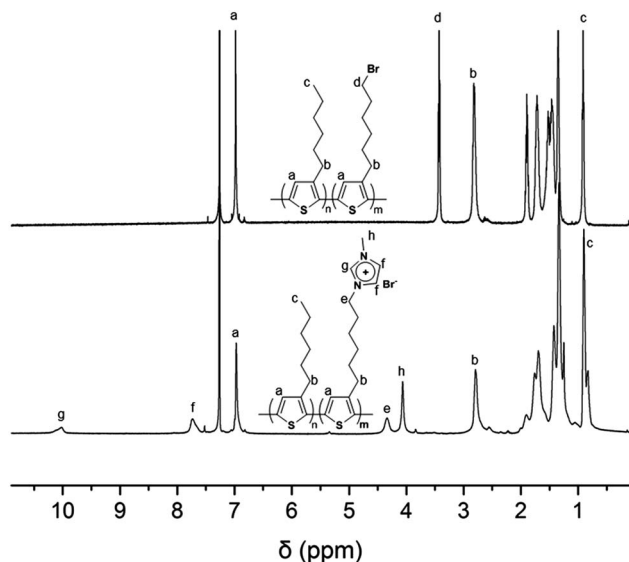

Fig. 2 ^{1}H NMR spectra of (a) P3HT-*b*-P3BrHT and (b) P3HT-*b*-P3MHT in CDCl$_3$.

P3HT-*b*-P3MHT with three different block ratios, and the corresponding homopolymers P3HT and P3MHT were measured by TGA (Fig. 3) and DSC (Fig. 4). TGA experiments were performed in two modes. In one mode, when the heating temperature was directly increased from room temperature to 700 °C, a weight loss below 100 °C was always found in P3MHT and P3HT-*b*-P3MHT samples although the samples were dried in
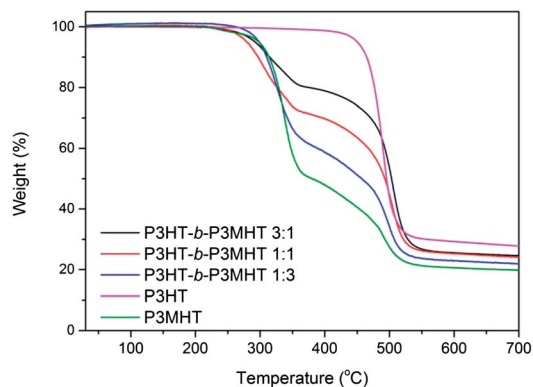

Fig. 3 TGA curves of P3HT, P3MHT and P3HT-*b*-P3MHT.
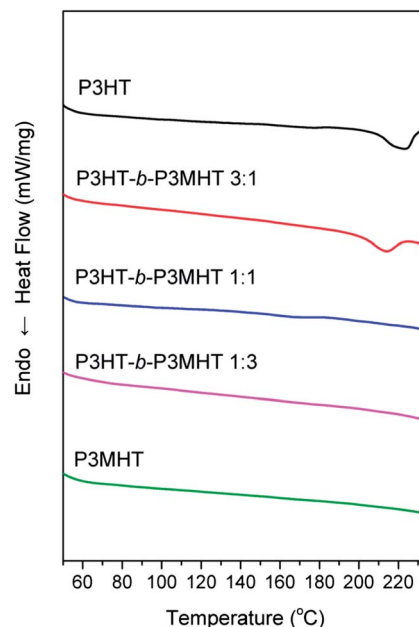

Fig. 4 DSC endotherms of P3HT, P3MHT and P3HT-*b*-P3MHT.

vacuum for more than 1 day before measurement (image not shown). The weight loss below 100 °C is due to the loss of the associated water with pendant ionic *N*-methylimidazolium groups and with the increased content of P3MHT, the amount of weight loss also increased due to the more associated water. This phenomenon is very similar to those of other conjugated polymers with polar amino or ammonium side groups, *etc.*[36,37] In the other mode, the samples were first heated to a little above 100 °C for 10 min, cooled to room temperature, and then heated to 700 °C. The final run without the weight loss below 100 °C was shown in Fig. 3. Compared with the degradation onset of P3HT homopolymer at 430 °C, the incorporation of the P3MHT block into P3HT has dramatically decreased the degradation onset to 260 °C. Therefore, the samples were heated to 240 °C in the following DSC measurement to avoid their degradation. As shown in Fig. 4, the melting temperature (T_m) of P3HT is 221 °C, but we didn't observe an obvious melting peak in P3MHT homopolymer. There are two possibilities. One is the P3MHT doesn't crystallize, the other is the melting point of P3MHT is beyond the heating temperature 240 °C. Compared with the T_m of P3HT homopolymers, the T_m of P3HT block decreases to 213 °C in the copolymer of P3HT : P3MHT = 3 : 1. For the copolymers of P3HT : P3MHT = 1 : 1 and 1 : 3, the melting peak of P3HT is almost invisible. This is due to the covalently bonded P3MHT block depressed the P3HT crystallization. However, it is not clear whether the P3MHT homopolymer or P3MHT block crystallize or not in DSC measurement.

XRD studies

To further investigate the crystalline structures of the polyelectrolyte diblock copolymers P3HT-*b*-P3MHT, XRD was performed on these copolymers and the corresponding homopolymers (Fig. 5). The XRD patterns of P3HT
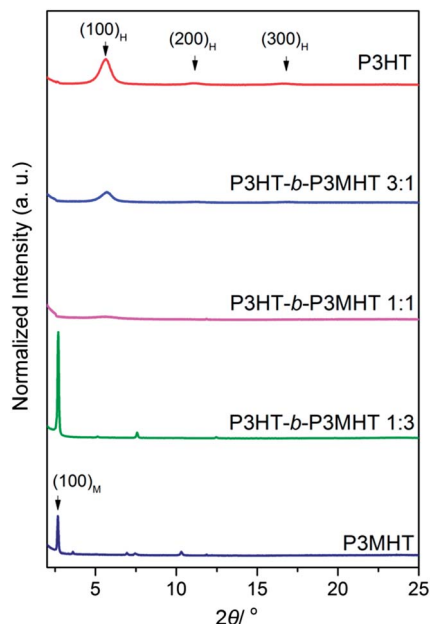
Fig. 5 XRD profiles of P3HT, P3MHT, and P3HT-*b*-P3MHT casted from 10 mg mL^{-1} polymer solution.

homopolymer shows the recognizable first-, second- and third-order reflections from crystallographic (100), (200) and (300) planes, respectively. The diffraction peaks at the 2θ angles of 5.9°, 11.5° and 17.0° correspond to the (100), (200) and (300) reflections of the P3HT homopolymer, respectively (denoted as (100)$_H$, (200)$_H$, and (300)$_H$ in Fig. 5). For P3MHT homopolymer, only the recognizable first-order reflection is shown from crystallographic (100) plane with the 2θ angle of 2.6° (denoted as (100)$_M$ in Fig. 5). We note a few other small peaks at 3.6°, 6.4°, 7.5°, and 10.2°, which may due to the Form II of P3MHT. These results indicate that both P3HT and P3MHT homopolymers crystallize into lamellar structure. The absence of melting peak of P3MHT homopolymer in DSC measurement is possibly due to the melting point of P3MHT is beyond its degradation temperature. Based on the (100)$_H$ and (100)$_M$ peaks, the interlayer spacings of the P3HT ($d_{100(H)}$) and P3MHT ($d_{100(M)}$) homopolymers are 15.0 Å and 33.1 Å, respectively.

It is notable that the interlayer spacing of P3MHT has about doubled after adding an imidazole group in the side chain. The doubling of the interlayer lattice periodicity of P3AT is also found in previous reports both experimentally[38] and theoretically,[39] although the (k00) reflections, when $k = 2n + 1$ ($n = 0, 1, 2\ldots$), are absent in the space group (*i.e. A2$_1$22*) when the side chains in a given layer are isodirectional packing.[40–44] The introduction of ionic group to the side chain of P3MHT in our system may lead the symmetry operators with a crystallographic 2_1 to be forbidden.[45] The absent of 2-fold screw conformation makes the observed reflection of P3MHT crystal not ever follow the law of disappeared (k00) reflections, resulting in the halving of 2θ angle of (100) reflection.[41] Therefore, the changed space group may indicate that the side chains of P3MHT in crystal are in asymmetric arrangement or random orientation, rather than in herringbone arrangement.

Compared with P3HT and P3MHT homopolymers, the crystalline structures of their diblock copolymers P3HT-*b*-P3MHT are influenced by their block ratios. In general, the major block in the copolymer dominates the crystalline structure while the crystalline behavior of the other minor block is effectively depressed. For the copolymer of P3HT : P3MHT = 3 : 1, one single (100) diffraction peak at the 2θ angle of 5.7° is observed, corresponding to the $d_{100(H)}$ value of 15.5 Å. For the copolymer of P3HT : P3MHT = 1 : 3, the (100) reflection at the 2θ angle of 2.7° is observed, corresponding to the $d_{100(M)}$ value of 32.8 Å. In both cases, the (100) diffraction peak of the other minor block is not observed. It demonstrates that there is an interplay between the crystallization of the P3HT and P3MHT blocks and the final crystalline structure that forms is determined to a large extent by the competition between them which crystallizes stronger, influenced by their relative content. The crystallization of the copolymer of P3HT : P3MHT = 3 : 1 and 1 : 3 is schematically shown in Fig. 6. These results are different from our previous study on P3AT-*b*-P3AT systems, in which cocrystallization was observed when their alkyl side chains were different by two carbon atoms while independent crystallization of each block was observed when their alkyl side chains were different by more than two carbon atoms.[20] Further investigation of the polyelectrolyte type of other all-conjugated P3AT-*b*-P3AT diblock copolymers is underway.
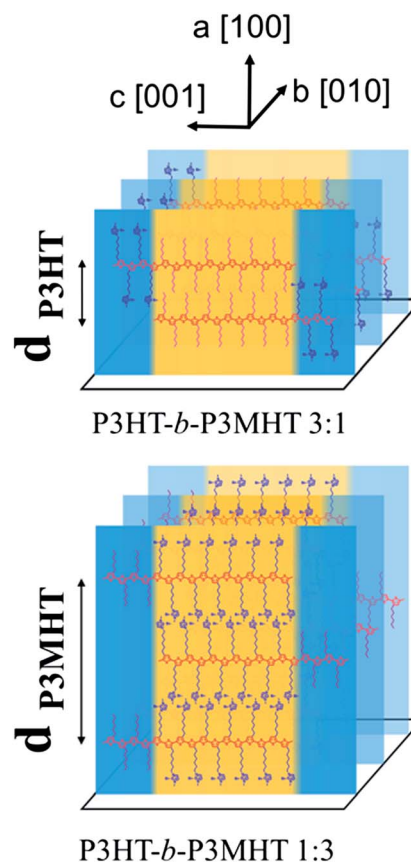

Fig. 6 Schematic representation of crystalline lamellar structures of P3HT-*b*-P3MHT (P3HT : P3MHT = 1 : 3 and 3 : 1) derived from XRD results.

Optical properties

The photophysical properties of the polyelectrolyte diblock copolymer P3HT-*b*-P3MHT were studied by UV-vis spectroscopy. Fig. 7 shows the normalized UV-vis spectra of P3HT-*b*-P3MHT with three different block ratios in methanol. Since methanol is a good solvent for P3MHT block but a poor solvent for P3HT block, the block ratios of P3HT to P3MHT greatly influences the aggregated structure of the copolymer in the solution. In general, the higher content of P3HT in the copolymer, the more aggregated structure forms in the methanol. One major absorption peak with a maximum at 443 nm is observed for the copolymer of P3HT : P3MHT = 1 : 3, which is typical for P3AT-type polymers due to the π–π* transition of the polythiophene main chain. It suggests that the copolymer of P3HT : P3MHT = 1 : 3 is well soluble in methanol, adopting the coil conformation. While for the copolymer of P3HT : P3MHT = 3 : 1, a bathochromic shift of the absorption spectrum was observed with the main peak at 515 nm and two vibronic peaks at 550 and 601 nm, respectively, which were attributed to the absorption of the strong interchain π–π interaction. It indicates the conformation of the copolymer of P3HT : P3MHT = 3 : 1 is the aggregated structure. For the copolymer of P3HT : P3MHT = 1 : 1, the UV-vis spectra located in the middle with the main peak at 473 nm.

Self-assembly behavior in solution

It is known that P3HT exist in two different conformations in the solution: a random coil conformation and a planarized conformation which is greatly influenced by the quality of the solvents used.[22] Methanol, water and chloroform were chosen as typical solvents in which methanol and water are P3MHT-selective solvents and chloroform is P3HT-selective. In the following, it shows that the P3HT-*b*-P3MHT morphology was quite dependent on the solvent selectivity for the two blocks and the block ratios. The aforementioned UV-vis spectra of the P3HT-*b*-P3MHT copolymer in methanol revealed that the block ratio has a marked effect on the photophysical properties. Now we show that such dis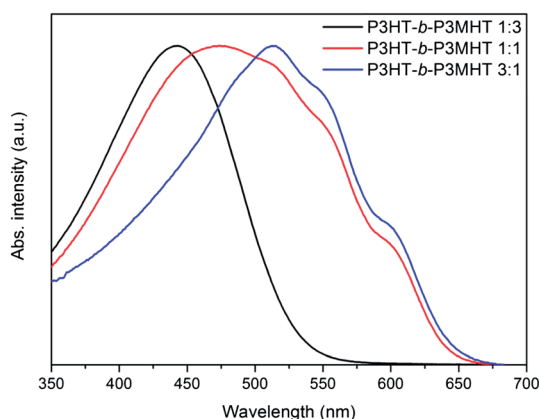tinctive solvatochromic changes are concomitant with the structural variations. For the copolymer of P3HT : P3MHT = 3 : 1, short nanowires formed in methanol with the length and width of 30–430 nm and 23 nm, respectively (Fig. 8a). Since methanol is a poor solvent to P3HT, the major P3HT blocks in the copolymer formed a planarized conformation against each other to form crystalline nanowires. For the copolymer of P3HT : P3MHT = 1 : 1, much less short nanowires was observed (Fig. 8b). For the copolymer of P3HT : P3MHT = 1 : 3, short nanowires disappeared and a flat surface with some nanodots were observed (Fig. 8c). The major P3MHT block makes the copolymer dissolve in methanol well and form a uniform surface. In addition to methanol, water was also used as the solvent for the study of self-assembly. Although both of them are selective solvents for P3MHT, different self-assembly behavior were observed between methanol and water. For example, for the copolymer of P3HT : P3MHT = 1 : 1, it formed isolated aggregates in which most of them were spherical in water (Fig. 8d). It reflected different conformation or nature of the copolymer present in the two solvents.

We then discuss the solution structures of P3HT-*b*-P3MHT copolymers in chloroform, which are quite different from the corresponding structures in methanol. As the copolymer of P3HT : P3MHT = 1 : 3 is not well-dissolved in chloroform, we only discuss solution structures of the other two copolymers. Compared with the short nanowires formed in methanol in the copolymer of P3HT : P3MHT = 3 : 1, it formed much longer nanowires in chloroform (Fig. 9a). The average length of the nanowires is 1.7 μm. The width of the nanowires is about 26–46 nm. For the copolymer of P3HT : P3MHT = 1 : 1, in addition to nanowires, nanorings emerged in the solution (Fig. 9b). The diameter of the nanorings is in the range of 90–350 nm with the

Fig. 7 UV-vis spectra of P3HT-*b*-P3MHT of various block ratios in methanol.
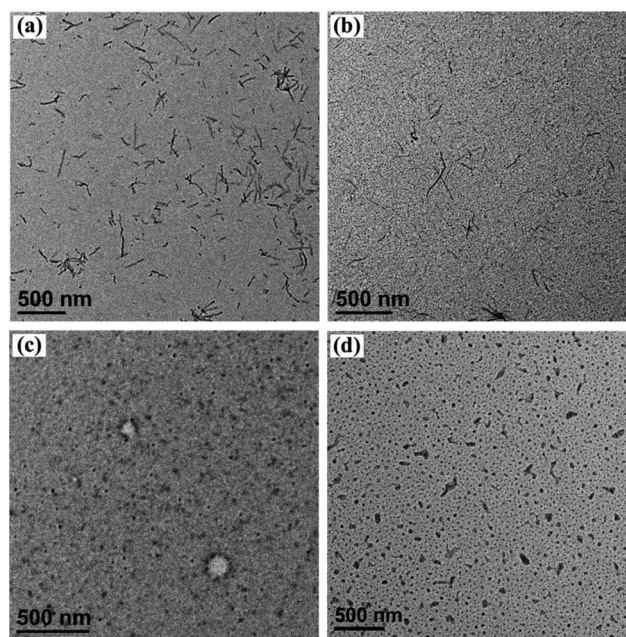

Fig. 8 TEM images of P3HT-*b*-P3MHT of various block ratios in P3MHT-selective solvents. (a–c) in methanol and (d) in water. The block ratio of P3HT to P3MHT is (a) 3 : 1, (b and d) 1 : 1, and (c) 1 : 3.
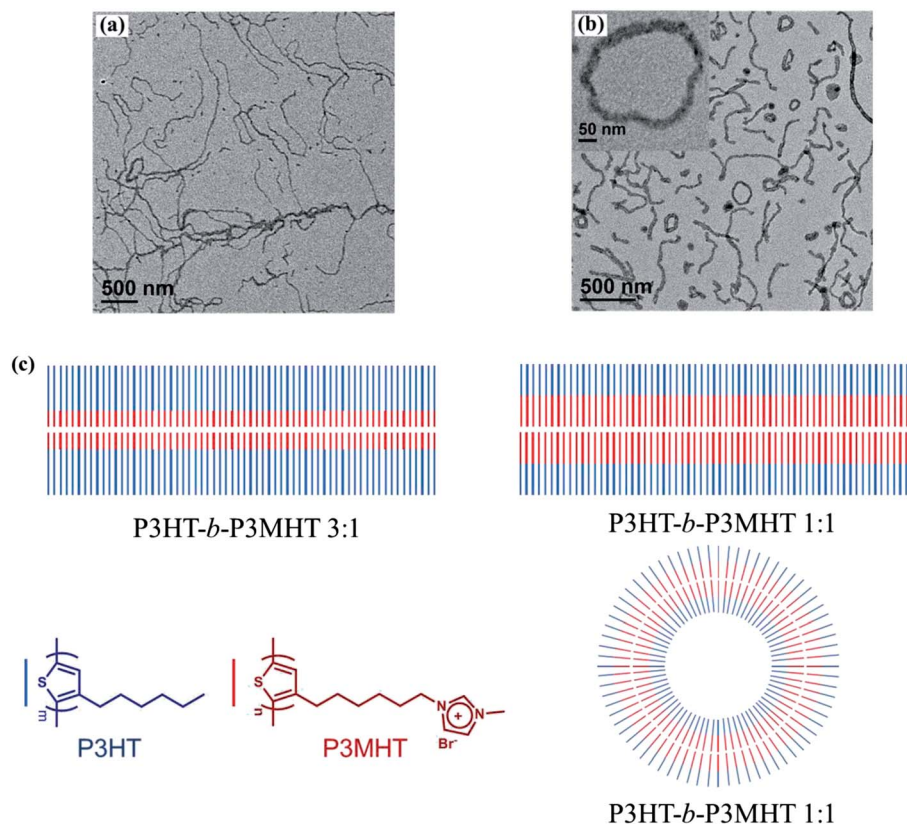
Fig. 9   TEM images of P3HT-*b*-P3MHT of various block ratios in chloroform. The block ratio of P3HT to P3MHT is (a) 3 : 1 and (b) 1 : 1. The inset of (b) is a magnified TEM image of a nanoring. (c) Schematic representation of the corresponding P3HT-*b*-P3MHT chains in chloroform.

ring width of 33–44 nm. Both nanowires and nanorings can be stably dispersed in the solution for a long time.

In the following we concentrate on the possible reason that leads to the formation of nanowires and nanorings in chloroform. It is clear that the polymer–solvent interaction plays a crucial role in the self-assembly of copolymer into long nanowires and nanorings. Since chloroform is a good solvent for P3HT block but poor for P3MHT block, P3HT-*b*-P3MHT can be viewed as an "amphiphilic" rod-coil block copolymer with a solvophilic coil-like of P3HT block and a solvophobic rod-like P3MHT block. As a result, P3HT-*b*-P3MHT copolymer packed into bilayer structure (long nanowires in Fig. 9a) with the P3MHT blocks inside and the P3HT blocks outside to minimize the unfavorable contacts between the solvophobic P3MHT block and chloroform. By calculation, a single copolymer chain in the fully stretched state is nearly 16 nm with the monomer length of 0.4 nm.[46] The average width of nanowires in Fig. 9a was approximately 32.6 nm, which supports the formation of a bilayer structure. For the copolymer of P3HT : P3MHT = 1 : 1, it has an increased content of P3MHT and thus lower solubility in chloroform. Consequently, the bilayer structure curled into nanorings to further reduce the unfavorable contacts between P3MHT and chloroform, and minimize the free energy of the system. The possible structures of nanowires and nanorings in chloroform are schematically shown in Fig. 9c.

Conclusions

In summary, we have synthesized a new class of all-conjugated polyelectrolyte diblock copoly(3-hexylthiophene)s *via* a well-established synthetic approach, *i.e.*, using a catalyst-transfer Kumada polycondensation and a subsequent quaternization step. The synthesis started from 2-bromo-5-iodo-3-hexylthiophene, which has good selectivity of activation and hence ensure the narrow PDI and high regioregularity. Their characterizations as well as thermal, crystalline, optical properties, and solution structure have been investigated in detail using NMR, GPC, DSC, TGA, XRD, and TEM. It is found that solvents and block ratios have great effects on the solution structure. A series of morphologies including short or long nanowires and nanorings could be obtained depending on the selectivity of solvents to different blocks and the block ratios. Future work will focus on the application of the polyelectrolyte diblock copoly(3-hexylthiophene)s in organic photovoltaic cells and related applications.

Acknowledgements

References

1 J. C. Bernède, *J. Chil. Chem. Soc.*, 2008, **53**, 1549–1564.

2 P. W. M. Blom, V. D. Mihailetchi, L. J. A. Koster and D. E. Markov, *Adv. Mater.*, 2007, **19**, 1551–1566.

3 S. Günes, H. Neugebauer and N. S. Sariciftci, *Chem. Rev.*, 2007, **107**, 1324–1338.

4 M. Muccini, *Nat. Mater.*, 2006, **5**, 605–613.

5 J. H. Burroughes, D. D. C. Bradley, A. R. Brown, R. N. Marks, K. Mackay, R. H. Friend, P. L. Burns and A. B. Holmes, *Nature*, 1990, **347**, 539–541.

6 I. Osaka and R. D. McCullough, *Acc. Chem. Res.*, 2008, **41**, 1202–1214.

7 C.-A. Dai, W.-C. Yen, Y.-H. Lee, C.-C. Ho and W.-F. Su, *J. Am. Chem. Soc.*, 2007, **129**, 11036–11038.

8 Y. J. Lee, S. H. Kim, H. Yang, M. Jang, S. S. Hwang, H. S. Lee and K.-Y. Baek, *J. Phys. Chem. C*, 2011, **115**, 4228–4234.

9 H. C. Moon, A. Anthonysamy, J. K. Kim and A. Hirao, *Macromolecules*, 2011, **44**, 1894–1899.

10 Z. Gu, T. Kanto, K. Tsuchiya, T. Shimomura and K. Ogino, *J. Polym. Sci., Part A: Polym. Chem.*, 2011, **49**, 2645–2652.

11 S. J. Park, S. G. Kang, M. Fryd, J. G. Saven and S. J. Park, *J. Am. Chem. Soc.*, 2010, **132**, 9931–9933.

12 H. Yang, H. Xia, G. W. Wang, J. Peng and F. Qiu, *J. Polym. Sci., Part A: Polym. Chem.*, 2012, **50**, 5060–5067.

13 U. Scherf, A. Gutacker and N. Koenen, *Acc. Chem. Res.*, 2008, **41**, 1086–1097.

14 G. L. Tu, H. B. Li, M. Forster, R. Heiderhoff, L. J. Balk, R. Sigel and U. Scherf, *Small*, 2007, **3**, 1001–1006.

15 Z. Q. Wu, R. J. Ono, Z. Chen, Z. Li and C. W. Bielawski, *Polym. Chem.*, 2011, **2**, 300–302.

16 J. Hollinger, A. A. Jahnke, N. Coombs and D. S. Seferos, *J. Am. Chem. Soc.*, 2010, **132**, 8546–8547.

17 M. C. Iovu, E. E. Sheina, R. R. Gil and R. D. McCullough, *Macromolecules*, 2005, **38**, 8649–8656.

18 P. T. Wu, G. Ren, C. Li, R. Mezzenga and S. A. Jenekhe, *Macromolecules*, 2009, **42**, 2317–2320.

19 P. T. Wu, G. Ren, F. S. Kim, C. Li, R. Mezzenga and S. A. Jenekhe, *J. Polym. Sci., Part A: Polym. Chem.*, 2010, **48**, 614–626.

20 J. Ge, M. He, F. Qiu and Y. Yang, *Macromolecules*, 2010, **43**, 6422–6428.

21 J. Ge, M. He, X. B. Yang, Z. Ye, X. F. Liu and F. Qiu, *J. Mater. Chem.*, 2012, **22**, 19213–19221.

22 M. He, L. Zhao, J. Wang, W. Han, Y. Yang, F. Qiu and Z. Lin, *ACS Nano*, 2010, **4**, 3241–3247.

23 Y. Song, J. Kim, M. J. Im, B. J. Moon and T. Park, *Macromolecules*, 2012, **45**, 5058–5068.

24 C. Ho, Y. Liu, S. Lin and W. Su, *Macromolecules*, 2012, **45**, 813–820.

25 X. H. Yu, H. Yang, S. Wu, Y. H. Geng and Y. C. Han, *Macromolecules*, 2012, **45**, 266–274.

26 Y. Zhang, K. Tajima, K. Hirota and K. Hashimoto, *J. Am. Chem. Soc.*, 2008, **130**, 7812–7813.

27 Y. Lin, J. A. Lim, Q. Wei, S. C. B. Mannsfeld, A. L. Briseno and J. J. Watkins, *Chem. Mater.*, 2012, **24**, 622–632.

28 C. Chue, T. Higashihara, J. Tsai, M. Ueda and W. Chen, *Org. Electron.*, 2009, **10**, 1541–1548.

29 S. Wu, L. Bu, L. Huang, X. H. Yu, Y. C. Han, Y. H. Geng and F. S. Wang, *Polymer*, 2009, **50**, 6245–6259.

30 K. Yao, L. Chen, Y. Chen, F. Li and P. Wang, *J. Mater. Chem.*, 2011, **21**, 13780–13784.

31 D. Bondarev, J. Zedník, I. Šloufová, A. Sharf, M. Procházka, J. Pfleger and J. Vohlídal, *J. Polym. Sci., Part A: Polym. Chem.*, 2010, **48**, 3073–3081.

32 X. Duan, L. Liu, F. Feng and S. Wang, *Acc. Chem. Res.*, 2010, **43**, 260–270.

33 A. Gutacker, S. Adamczyk, A. Helfer, L. E. Garner, R. C. Evans, S. M. Fonseca, M. Knaapila, G. C. Bazan, H. D. Burrows and U. Scherf, *J. Mater. Chem.*, 2010, **20**, 1423–1430.

34 A. Gutacker, C.-Y. Lin, L. Ying, T.-Q. Nguyen, U. Scherf and G. C. Bazan, *Macromolecules*, 2012, **45**, 4441–4446.

35 A. Yokoyama, R. Miyakoshi and T. Yokozawa, *Macromolecules*, 2004, **37**, 1169–1171.

36 B. Liu, W. L. Yu, Y. H. Lai and W. Huang, *Macromolecules*, 2002, **35**, 4975–4982.

37 F. Huang, H. Wu, D. Wang, W. Yang and Y. Cao, *Chem. Mater.*, 2004, **16**, 708–716.

38 T. J. Prosa, M. J. Winokur, J. Moulton, P. Smith and A. J. Heeger, *Macromolecules*, 1992, **25**, 4364–4372.

39 T. Tsumuraya, J. H. Song and A. J. Freeman, *Phys. Rev. B: Condens. Matter Mater. Phys.*, 2012, **86**, 075114.

40 P. Arosio, M. Moreno, A. Famulari, G. Raos, M. Catellani and S. V. Meille, *Chem. Mater.*, 2009, **21**, 78–87.

41 P. Arosio, A. Famulari, M. Catellani, S. Luzzati, L. Torsi and S. V. Meille, *Macromolecules*, 2007, **40**, 3–5.

42 K. Tashiro, M. Kobayashi, T. Kawai and K. Yoshino, *Polymer*, 1997, **38**, 2867–2879.

43 K. Tashiro, M. Kobayashi, S. Morita, T. Kawai and K. Yoshino, *Synth. Met.*, 1995, **69**, 397–398.

44 K. Tashiro, K. Ono, Y. Minagawa, M. Kobayashi, T. Kawai and K. Yoshino, *J. Polym. Sci., Part B: Polym. Phys.*, 1991, **29**, 1223–1233.

45 N. Kayunkid, S. Uttiya and M. Brinkmann, *Macromolecules*, 2010, **43**, 4961–4967.

46 S. Samitsu, T. Shimomura, S. Heike, T. Hashizume and K. Ito, *Macromolecules*, 2008, **41**, 8000–8010.